

Applications of deep learning for detecting ophthalmic diseases with ultrawide-field fundus images

Qing-Qing Tang¹, Xiang-Gang Yang¹, Hong-Qiu Wang², Da-Wen Wu¹, Mei-Xia Zhang¹

¹Department of Ophthalmology and Research Laboratory of Macular Disease, West China Hospital, Sichuan University, Chengdu 610041, Sichuan Province, China

²Hong Kong University of Science and Technology (Guangzhou), Guangzhou 511400, Guangdong Province, China

Co-first authors: Qing-Qing Tang and Xiang-Gang Yang

Correspondence to: Mei-Xia Zhang, Department of Ophthalmology and Research Laboratory of Macular Disease, West China Hospital, Sichuan University, Chengdu 610041, Sichuan Province, China. zhangmeixia@scu.edu.cn

Received: 2023-03-04 Accepted: 2023-11-07

Abstract

• **AIM:** To summarize the application of deep learning in detecting ophthalmic disease with ultrawide-field fundus images and analyze the advantages, limitations, and possible solutions common to all tasks.

• **METHODS:** We searched three academic databases, including PubMed, Web of Science, and Ovid, with the date of August 2022. We matched and screened according to the target keywords and publication year and retrieved a total of 4358 research papers according to the keywords, of which 23 studies were retrieved on applying deep learning in diagnosing ophthalmic disease with ultrawide-field images.

• **RESULTS:** Deep learning in ultrawide-field images can detect various ophthalmic diseases and achieve great performance, including diabetic retinopathy, glaucoma, age-related macular degeneration, retinal vein occlusions, retinal detachment, and other peripheral retinal diseases. Compared to fundus images, the ultrawide-field fundus scanning laser ophthalmoscopy enables the capture of the ocular fundus up to 200° in a single exposure, which can observe more areas of the retina.

• **CONCLUSION:** The combination of ultrawide-field fundus images and artificial intelligence will achieve great performance in diagnosing multiple ophthalmic diseases in the future.

• **KEYWORDS:** ultrawide-field fundus images; deep learning; disease diagnosis; ophthalmic disease

DOI:10.18240/ijo.2024.01.24

Citation: Tang QQ, Yang XG, Wang HQ, Wu DW, Zhang MX. Applications of deep learning for detecting ophthalmic diseases with ultrawide-field fundus images. *Int J Ophthalmol* 2024;17(1):188-200

INTRODUCTION

With the aging population, the number of patients with ophthalmic disease is increasing progressively. According to the report released by the World Health Organization in October 2019, more than 2.2 billion people have vision impairment or blindness worldwide, of whom at least 1 billion have vision impairment^[1]. Among them, fundus disease is one of the leading causes of severe vision impairment and blindness, and diabetic retinopathy (DR) is one of the most common severe diseases secondary to diabetes^[2]. By 2030, the global prevalence of diabetes is estimated to rise to 10.2%^[3], age-related macular disease (AMD) will increase 1.2 times^[4] compared with 2020 (195.6 million). The number of people with glaucoma is expected to increase to 111.8 million by 2040^[5], a 1.47-fold increase from 2020. Similarly, more patients with pathological myopia (PM) will lose vision^[6]. However, many patients with eye diseases cannot receive adequate medical diagnosis and treatment due to the insufficiency of medical resources. It often causes irreparable visual damage and increases the severe financial burden on patients and society. Therefore, the early screening, diagnosis, and treatment of eye diseases are particularly critical. To some extent, the development of artificial intelligence (AI) to assist in diagnosing ophthalmic diseases will significantly alleviate this situation.

In the field of ophthalmology, deep learning (DL) has been used in various image data, including color fundus photography (CFP)^[7-8], optical coherence tomography (OCT)^[9], optical coherence tomography angiography (OCTA)^[10-11], fundus fluorescein angiography (FFA) and ultrawide-field fundus (UWF) images^[12-13]. CFP images are the most critical research object, concentrating on diagnosing DR, AMD, glaucoma, *etc*^[7-8,14]. In recent years, the detection of macular lesions by OCT images has also gradually increased, such as macular edema (ME)^[15-16], epiretinal membrane^[17], macular hole^[18], and high myopia^[19]. Compared to traditional fundus cameras, UWF imaging technology can provide a wider field of

retina. However, there are relatively few studies based on UWF images, mainly because it is a relatively new device technology that has not been widely applied in hospitals and ophthalmology clinics. Therefore, it is essential to summarize the application of DL in detecting ophthalmic disease with UWF images in recent years, combined with the limitations and possible solutions common to all tasks.

Ultrawide-Field Fundus Images The UWF imaging system is classified into several categories: Optos and Heidelberg Spectralias/Heidelberg Retinal Angiography (HRA) cSLO. Clarus, Staurengi, RetCam and Panoret-1000™^[20-21]. The majority of UWF images thus far have been obtained with the Optos, which has allowed the capture of 200° of the retinal range (approximately 82% of the retina) in one shot without mydriasis^[20,22] (Figure 1). The Optos imaging device uses pseudocolor combined with the red and green laser wavelengths, and the green (red-free) component depicts the retina and its vasculature. In contrast, the red component highlights deeper structures^[21]. Furthermore, it is also called an ultrawide-filed pseudocolor (UWPC) image or scanning laser ophthalmoscope (SLO) image. Therefore, the application of DL in UWF images also mainly focused on Optos images according to the research, so the remainder of UWF images in this review will refer to the Optos images mainly.

Deep Learning in Ophthalmic Diseases Based on Ultrawide-Field Fundus Images We searched three academic databases, including PubMed, Web of Science, and Ovid, with the date of August 2022. We matched and screened according to the target keywords and publication year and retrieved a total of 4358 research papers according to the keywords, of which 562 duplicated studies were excluded. Among the remaining articles, 3754 without keywords were filtered out by title and abstract. Fifty-one full-text articles were found to report the application of DL in ophthalmology with UWF images. Among them, 23 studies were retrieved on applying DL in diagnosing ophthalmic disease with UWF images (Figure 2). These include DR, glaucoma, AMD, retinal detachment (RD), retinal vein obstruction (RVO), *etc* (Figure 3).

Single Ophthalmic Disease

Diabetic retinopathy DR, a vascular disease of the eye, has emerged as one of the principal causes of vision impairment and blindness throughout the world^[23]. Prompt diagnosis and timely treatment of DR has been proven to save blindness^[24]. The high risk of DR in people with diabetes makes regular eye exams necessary. However, it is impractical and expensive for ophthalmologists to perform fundus examinations for all diabetic patients, given the shortage of ophthalmologists and the essential medical infrastructure required for the examinations^[13]. For this reason, AI, particularly DL, promises to provide a better solution for screening and diagnosis.

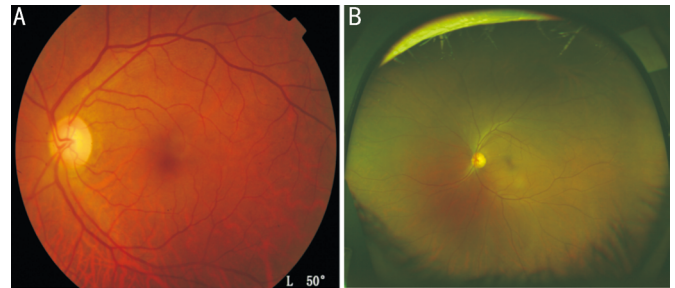


Figure 1 Color fundus (A) and ultrawide-field fundus (B) images.

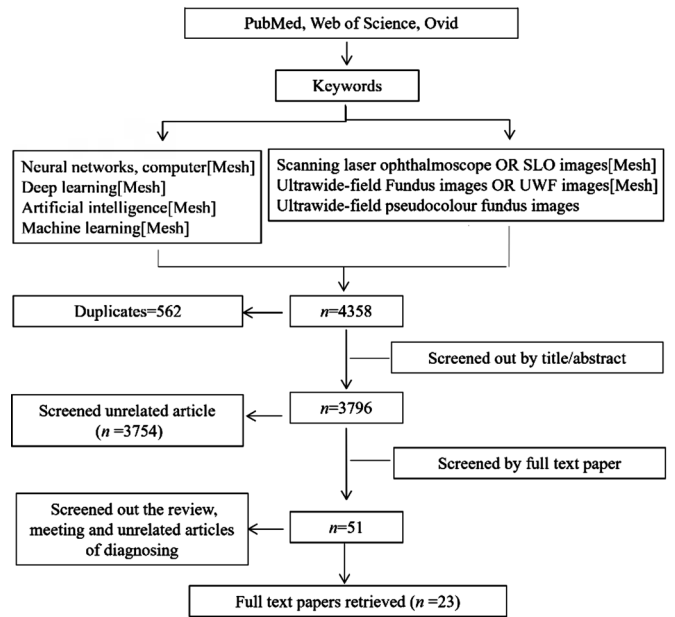


Figure 2 Process of searching and selecting studies for the review.

Historically, AI models for diagnosing DR have used standard fundus cameras that provide 30° to 50° images. However, the development of the UWF imaging fundus camera has become more beneficial to understanding and managing DR. This section provides the most comprehensive review of AI related to DR diagnosis based on UWF images, focusing on the methodological features, the clinical value of UWF images, and DL diagnostic models. A summary of the essential characteristics of the included studies is shown in Table 1. The International Clinical Diabetic Retinopathy Scale (ICDRS) is a unified standard for the classification of DR, and is currently used in most DL studies. According to this criterion, it can classify the severity of DR into five levels: level 0 (no significant DR), level 1 (mild DR), level 2 (moderate DR), level 3 (severe DR), and level 4 (proliferative DR)^[24-25]. In DL related to DR diagnosis based on UWF images, even though the Early Treatment Diabetic Retinopathy Study (ETDRS) is considered a gold standard in diagnosing DR^[26-27], it may be appropriate to use ICDRS as a standard in evaluating AI screening systems. There are two reasons. First, given the easier and broader application of ICDRS in daily clinical work. Second, a systematic review has shown that the diagnostic accuracy of neural networks might not be affected

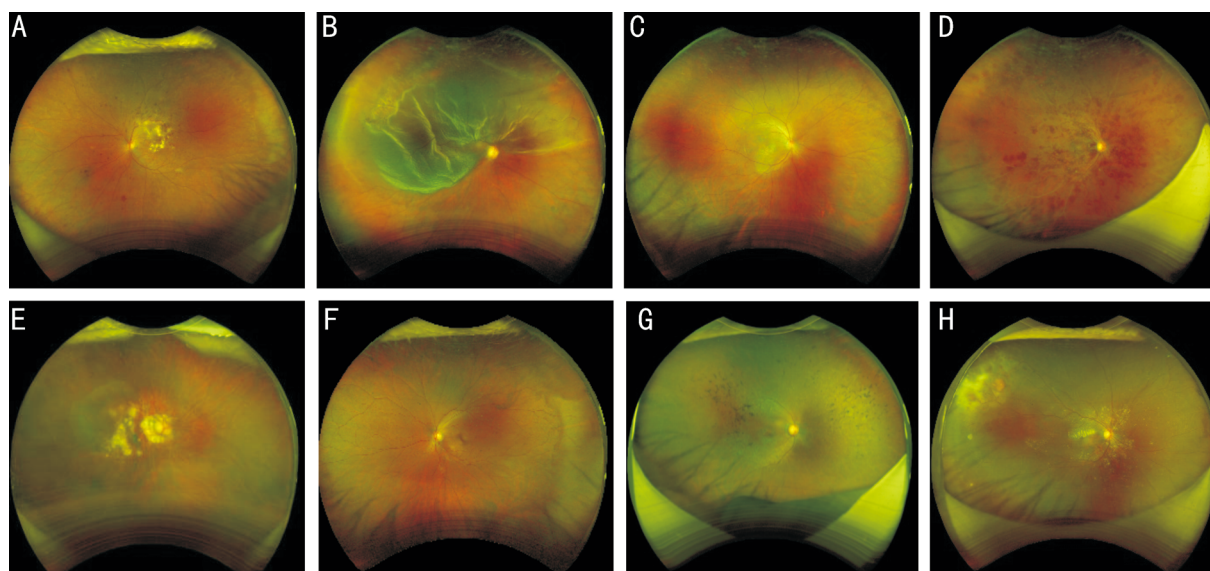


Figure 3 Different disease in ultrawide-field fundus images diagnosed by deep learning A: Diabetes retinopathy; B: Retinal detachment; C: Age-related macular degeneration; D: Retinal vein obstruction; E: Pathologic myopia; F: Lattice degeneration; G: Retinitis pigmentosa; H: Coats.

Table 1 Research work reported for diagnosis of DR with DL using UWF images

Author, y	Country	Study design	Image number	Tested disease	Diagnostic criteria	Methods	Group	Results
Nagasawa <i>et al</i> , 2021	Japan	Retro.	UWF: 491; OCTA: 491	NDR vs DR; NDR vs PDR	ETDRS	VGG-16	NDR and DR	UWF AUC=0.79, SE=80.9%, SP=55.0%
							OCTA	AUC=0.88, SE=83.9%, SP=71.6%
							UWF OCTA	AUC=0.847, SE=78.6%, SP=69.8%
							NDR and PDR	UWF AUC=0.981, SE=90.2%, SP=97.0%
							OCTA	AUC=0.928, SE=74.5%, SP=97.0%
UWF OCTA	AUC=0.964, SE=80.4%, SP=96.4%							
Nagasawa <i>et al</i> , 2019	Japan	Retro.	UWF: 378	PDR vs non-PDR	ETDRS		AUC=0.969, SE=94.7%, SP=97.2%	
Wang <i>et al</i> , 2018	India	Retro.	UWF: 1661	Referral-warranted DR vs normal	ICDRS	EyeArt algorithm	Patient levels	AUC=0.873, SE=91.7%, SP=50.0%
							Eye levels	AUC=0.851, SE=90.3%, SP=53.6%
Oh <i>et al</i> , 2021	Korea	Retro.	UWF: 13271	DR vs non-DR	ETDRS	ResNet-34, U-Net	ETDRS 7SF	AUC=0.915, SE=83.4%, SP=83.4%, ACC=83.4%
							ETDRS F1–F2 fundus images	AUC=0.887, SE=80.6%, SP=80.6%, ACC=80.6%

DL: Deep learning; UWF: Ultrawide-field fundus; OCTA: Optical coherence tomography angiography; DR: Diabetic retinopathy; NDR: No apparent diabetic retinopathy; PDR: Proliferative diabetic retinopathy; ETDRS: Early Treatment Diabetic Retinopathy Study; VGG-16: Visual Geometry Group Network with 16-layer; SLO: Scanning laser ophthalmoscopy; RP: Retinitis pigmentosa; ResNet-34: Residual Network with 34-layer; ICDRS: International Clinical Diabetic Retinopathy score; AUC: Area under curve; SE: Sensitivity; SP: Specificity; ACC: Correct answer rate.

by the criteria used in ophthalmologists’ diagnosis, and the ICDRS as the diagnostic criterion has also achieved good results as well as others, which is probably because ICDRS was developed on ETDRS^[26]. Nagasawa *et al*^[28] proposed a system that can perform binary classification of proliferative diabetic retinopathy (PDR) using 378 resized and normalized UWF images. It applied Visual Geometry Group Network with 16 layers (VGG-16) to classify DR. The sensitivity, specificity,

and area under the curve (AUC) of the DL model were 94.7%, 97.2%, and 96.9%, respectively. Two years later, Nagasawa *et al*^[13] also used VGG-16 and data preprocessing methods to detect DR with 491 UWF images, 491 OCTA images, and 491 UWF-OCTA images generated vertically by combining UWF and OCTA images. All images were graded into five types: no apparent DR (NDR), mild nonproliferative DR (NPDR), moderate NPDR, severe NPDR, and proliferative

DR (PDR) by three retinal experts using the ETDRS. The metrics of “NDR and DR” and “NDR and PDR” are shown in Table 1. To the best of our knowledge, this is the first study to combine UWF and OCTA imaging with DL, showing the great potential of multimodal with DL. Although combining multiple imaging techniques may overcome the weaknesses and provide comprehensive information, DL does not always produce accurate results when classifying multimodal images, foreshadowing that there is still tremendous room for research in this area.

The ETDRS 7-standard field (7SF) is the most significant region of UWF fundus photography. Oh *et al*^[29] restricted the region of interest to the ETDRS 7SF for the DR detection task based on UWF fundus photography. First, they extracted the ETDRS 7-SF based on the optic disc and macula centers utilizing the U-Net model with the pretrained residual network with 18 layers (ResNet-18). Next, they perform the classification task using a pretrained and finetuned ResNet-34 model to demonstrate the effectiveness of the automated DR detection. They also compared the DR detection performance of their system with that of a system based on the ETDRS F1-F2 images and the results better results were obtained. This study provides a new perspective for mining the clinical value of UWF images. Their DL model consists of a multibranch network, an atrous spatial pyramid pooling module (ASPP), and a cross-attention and depthwise attention module. Experiments conducted that their approach is superior to the current state-of-the-art methods^[29]. Gradient-weighted class activation mapping (Grad-CAM) visualization is used to visualize the essential features learned by the DL models to analyze the DL models' attention area, which enhancing the interpretability of DL models.

The corporate world is also paying close attention to the area of AI related to DR diagnosis based on UWF images. As commercial software, EYEART was first applied to the 1661 UWF images in 2018 to automatically quantify various DR lesions (lipid exudates, hemorrhage, microaneurysms, cotton wool spots), which was used to determine the level of DR and define each image as a referral or nonreferral^[30]. NPDR graded to be moderate or higher on the 5-level ICDRS is considered grounds for the referral. Year software was released in 2021 with version 2.1.014, which combines the DR detection algorithm of version 1.2 with the architecture of the DL networks. Although the image processing techniques of the EYEART algorithm are proprietary and not publicly available, the software has shown increasingly better performance through multiple rounds of validation and iteration on real-world datasets^[31].

Glaucoma Glaucoma is a disease characterized by optic disc cupping and visual field impairment resulting in irreversible

blindness globally^[32]. Usually, the patient is frequently undiagnosed until very late stages when central visual acuity is compromised. However, detecting glaucoma at an early stage is challenging because patients with glaucoma are often asymptomatic. Effective detection methods are necessary for large-scale screenings to identify glaucoma as early as possible. One report has suggested that we could use the UWF images (Optos) to identify glaucoma at an early stage with their high reproducibility. In 2018, Masumoto *et al*^[33] used UWF images to detect open angle glaucoma (OAG) characteristics and their severity with a CNN architecture, which was best for severe OAG. Nevertheless, a 25° box image centered on the optic disc and immediate surroundings might suffice to detect glaucoma. Hence, we need to determine whether classifiers trained on 200° images perform the same, better, or worse than classifiers trained on the central 25° images in the UWF images. Tabuchi *et al*^[34] proposed investigating the possibility of improving the ability of deep convolutional neural networks (DCNNs) to diagnose glaucoma using UWF images. In this study, VGG-16 was conducted to examine the ability to discriminate glaucoma with the whole area of UWF images (Full) and the partial area surrounding the optic disc (Cropped), and they trimmed the Cropped data roughly to the area containing the optic disc using a U-Net network. For the full dataset, the AUC was 0.987, the sensitivity was 0.957, and the specificity was 0.947. For the cropped dataset, the AUC was 0.93, the sensitivity was 0.868, and the specificity was 0.894. Their results showed that the whole UWF images were more appropriate as the amount of information given to a neural network for the discrimination of glaucoma than only the range limited to the periphery of the optic disc. Recently, Li *et al*^[35] developed an InceptionResNetV2 neural network architecture as a DL system for automated glaucomatous optic neuropathy (GON) detection based on 22 972 UWF images from 10 590 subjects collected at four different institutions in China and Japan. The system for GON detection achieved significant progress in automated GON detection. It can be used for automated central fundus lesion detection, even in external datasets (collected by different types of cameras) from subjects with various ethnic backgrounds in two countries. In 2022, Shin *et al*^[36] evaluated and compared the performance of UWF imaging and true-color confocal scanning images in detecting glaucoma based on the DL classifier. They found that the ability of DL-based UWF imaging and true-color confocal scanning to diagnose glaucoma was comparable to that of the OCT parameter-based method. Their analysis showed no significant difference in glaucoma diagnosis between the two modalities. However, as the study only used a limited dataset (small sample size), the results of the DL are inferior to the studies with large sample sizes (Table 2).

Table 2 Research work reported for diagnosis of other ophthalmic diseases except for DR with DL using UWF images

Author, y	Country	Disease	Image number	Methods	Group	Results	Machine type
Tabuchi <i>et al</i> , 2018	Japan	Glaucoma	2627	VGG16	The full data set	AUC=0.987, SE=0.957, SP=0.947	Optos
Masumoto <i>et al</i> , 2018	Japan	OAG	1399	CNN	The cropped data set	AUC=0.937, SE=0.868, SP=0.894	Optos
					Normal vs all glaucoma	AUC=0.872, SE=0.813, SP=80.2	
					Normal vs early OAG	AUC=0.83, SE=0.838, SP=0.753	
Li <i>et al</i> , 2021	China	Glaucomatous optic neuropathy	22972	InceptionResNetV2	Normal vs moderate OAG	AUC=0.864, SE=0.775, SP=0.902	Optos
					Normal vs severe OAG	AUC=0.934, SE=0.909, SP=0.958	
					China, CMAAI	AUC=0.999	
Shin <i>et al</i> , 2022	Korea	Glaucoma	777 eyes	VGG-19	South-east of China	AUC=0.983	Optos
					North-west of China	AUC=0.99	
					Japan	AUC=0.99	
Matsuba <i>et al</i> , 2019	Japan	Wet AMD	364	DCNN	UWF imaging	AUC=0.904, ACC=0.836	Optos/Eidon AF™
					True-color confocal scanner	AUC=0.868, ACC=0.814	
Tak <i>et al</i> , 2021	America	Exudative AMD	957	CNN	Exudative AMD	ACC=1 of left, ACC=0.818 of right, ACC=1 of bilateral eyes	Optos
Nagasato <i>et al</i> , 2018	Japan	CRVO	363	VGG-16	Non-exudative AMD	ACC=0.923 of left, ACC=1 of right, ACC=0.696 of bilateral eyes	Optos
					DL	AUC=0.989, SE=0.984, SP=0.979	
Nagasato <i>et al</i> , 2019	Japan	BRVO	466	VGG-16	DL	AUC=0.976, SE=0.94, SP=0.97	Optos
Ohsugi <i>et al</i> , 2017	Japan	RRD	649	CNN	SVM	AUC=0.835, SE=0.805, SP=0.843	Optos
					DL	AUC=0.988, SE=0.976, SP=0.965	
Li <i>et al</i> , 2020	China	RD	10451	Inception ResNet	RD and non-RD	AUC=0.976, SE=0.975, SP=0.893	Optos
					macula on RD	AUC=0.989, SE=0.954, SP=0.998	
Masumoto <i>et al</i> , 2019	Japan	Macula on and off RD	1771	VGG-16	UWF images	AUC=0.917, SE=0.938, SP=0.909	Optos
					UWFA images	AUC=1, SE=1, SP=0.995	
Nagasawa <i>et al</i> , 2018	Japan	Idiopathic macular holes	910	CNN	MHs and normal	AUC=0.999, SE=1, SP=0.995	Optos
Li <i>et al</i> , 2020	China	Retinal hemorrhage	16827	InceptionResNetV2	CMAAI	AUC=0.999, SE=0.995, SP=0.994, ACC=0.993	Optos
			905		ZOC	AUC=0.998, SE=0.967, SP=0.987, ACC=0.984	
			1236		Xudong Ophthalmology Hospital	AUC=0.997, SE=0.976, SP=0.98, ACC=0.98	
Li <i>et al</i> , 2019	China	Peripheral retinal lesions	5005	InceptionResNetV2	InceptionResNetV2	AUC=0.991, SE=0.987, SP=0.992	Optos
					InceptionV3	AUC=0.987, SE=0.987, SP=0.987	
					ResNet50	AUC=0.989, SE=0.968, SP=0.976	
					VGG16	AUC=0.998, SE=0.991, SP=0.985	

DR: Diabetic retinopathy; DL: Deep learning; AUC: Area under curve; SE: Sensitivity; SP: Specificity; ACC: Correct answer rate; OAG: Open angle glaucoma; UWF: Ultrawide-field; AMD Age-related macular degeneration; CRVO: Central retinal vein occlusion; BRVO: Branch retinal vein occlusion; RRD: Rhegmatogenous retinal detachment; RD: Retinal detachment; CMAAI: Chinese Medical Alliance for Artificial Intelligence.

Age-related macular degeneration It has been reported that AMD is one of the most common blindness diseases among the elderly in developed countries^[37-38]. With the development

of the disease, it leads to visual distortion and central vision decline. According to the specific characteristics of the disease, AMD can be divided into neovascular AMD (wet AMD) and

nonneovascular macular degeneration (dry AMD)^[37]. The long-term visual prognosis following anti-VEGF therapy depends on the patient's age and visual acuity at treatment initiation^[37,39]. Thus, ophthalmic consultation and appropriate treatment at an early stage are essential for patients. In 2019, Matsuba *et al*^[40] evaluated the diagnostic accuracy of AMD with 364 UWF images (AMD: 137). The DCNN exhibited 100% sensitivity and 97.31% specificity for wet AMD images with an average AUC of 99.76%, which is superior to the diagnostic abilities of six ophthalmologists (accuracy: 81.9%). Although the study achieved good performance in diagnosing wet AMD, they excluded cases with unclear images attributed to vitreous hemorrhage, astrocytosis, or strong cataracts. In addition, issues with previous retinal photocoagulation and other complicating ophthalmic diseases as determined by retinal specialists were not included. In 2021, Tak *et al*^[41] used a CNN to differentiate the exudative and nonexudative AMD with UWF images and determined whether the disease was present in the right, left, or both eyes with a relatively high degree of accuracy. One of the biggest strengths of this study is that the AI software utilized low-quality images and raw unprocessed clinical data to identify patterns and produce results. Unlike previous studies that were performed using processed images and datasets, AI will be more applicable to the practical clinical setting. Although UWF images can be used for the recognition and diagnosis of AMD, the accuracy for diagnosis of AMD in UWF images is insufficient compared with CFP and OCT, which may be related to some small lesions that are difficult to detect in UWF images at the early stage of AMD.

Retinal detachment and peripheral retinal lesions RD is a disease of detachment between the retinal neuroepithelial layer and pigmented epithelial layer. Rhegmatogenous RD (RRD) is the most common type of RD, with an incidence rate of approximately 1/10 000^[42-43]. RRD is a highly curable condition if adequately treated early, and the early diagnosis and treatment of other types of RD are also crucial. However, it is difficult to conduct a thorough examination of the peripheral retina without the professional vitreoretinal skills of ophthalmologists and pupil dilation of the patients. Hence, the advancement of UWF images provides a highly efficient modality for peripheral retina screening. It is possible to detect RD automatically using UWF images with the development of DL. In 2017, Ohsugi *et al*^[43] compared the application of DL and support vector machine (SVM) in RRD based on Optos fundus photographs. Their results showed that the DL technology for detecting RRD had high sensitivity of 97.6% and specificity of 96.5%. Although their results demonstrated great classification performance in diagnosing RRD, they excluded Optos images influenced by severe cataracts or dense vitreous hemorrhage (411 RRD images, 420 normal images).

Additionally, this study only compared the images of normal eyes and RRD. It did not include eyes with any other types of RD and ophthalmic diseases, which will not perform the real ability to diagnose RD by DL models. Three years later, Li *et al*^[44] explored DL for detecting RD (RRD, exudative RD, and tractional RD) using 11 087 UWF images, which improved the limitations mentioned above and showed great performance. Meanwhile, they probed the ability of discerning macula-on RD from macula-off RD with ideal performance. Moreover, they also developed a DL system for automated identification of notable peripheral retinal lesions (NPRLs), including lattice degeneration and retinal breaks, based on UWF images^[45]. This study verified the performance of 4 different DL algorithms (InceptionResNetV2, InceptionV3, ResNet50, and VGG-16) with 3 preprocessing techniques as original, augmented, and histogram-equalized images. They found that the best preprocessing method in each algorithm was the application of original image augmentation. A possible explanation is that augmentation turns each image into several images of various conditions. Therefore, the sample size is increased, which enables the generalization of the DL system to unseen data. Compared to other DL algorithms, the best algorithm in each preprocessing method was InceptionResNetV2, which could represent a more complex relationship between the input (UWF image) and output (the label we attempt to predict). Meanwhile, InceptionResNetV2 can reduce the tendency of overfitting by mimicking the skip connections from ResNet in large work. However, lattice degeneration and retinal breaks were not classified independently due to the small retinal breaks that often emerged within lattice degeneration; it is difficult to differentiate retinal breaks from lattice degeneration. Later, another study detected lattice degeneration, retinal breaks, and RD using UWF images with CNN, which will be discussed later in the application of DL in diagnosing multiple diseases^[46].

Other diseases In addition, DL has been used in a few studies on other diseases, such as RVO, retinitis pigmentosa (RP) and macular holes (MHs). RVO can be divided into central retinal vein occlusion (CRVO) and branch retinal vein occlusion (BRVO). It is considered as the second most frequent type of retinal vascular disorder^[47]. Nagasato *et al*^[48-49] applied VGG-16 and SVM in CRVO and BRVO classification and compared them in 2018 and 2019, respectively, in which the SVM is a machine learning method showing advantages in solving small samples. Although the DL model outperformed the SVM model, the limitation is that only one classification CRVO or BRVO in RVO has been studied in a single study. In addition, RVO has not been reclassified after a comprehensive study and has not been included in the studies. In 2019, Masumoto *et al*^[50]

evaluated the discrimination ability of a deep convolution neural network based on VGG-16 for UWPC imaging and ultrawide-field autofluorescence (UWAF) of RP (150 RP, 223 normal). RP is one of the most frequent hereditary diseases of the retina, mainly due to the dystrophy of cone and rod photoreceptor cells^[51-52]. Although the study concluded that the sensitivity for UWAF images was expected to be higher than that for UWPC images, there was no significant difference between them. The sensitivity and specificity in UWPC images are mainly close to 100%. Another study explored the ability of DL to diagnose idiopathic MHs with 715 normal images and 195 MH images^[53]. Their findings suggested that MHs could be diagnosed with a high sensitivity of 100% and a high specificity of 99.5% using UWF images. However, the lesions of MHs are a small part of the retina in UWF images; we cannot ignore the influence of cataracts, vitreous opacities, and retinal hemorrhage, which will greatly influence the performance of MHs in UWF images. Additionally, whether it can be detected from multiple diseases with panretinal disease is still a problem. At the same time, compared with DR, glaucoma, AMD and other diseases, the incidence of these diseases has decreased, and the number of UWF images based on DL studies is also small, so there may be overfitting problems in these DL studies with small samples.

Furthermore, Li *et al*^[54] mainly focused on classifying retinal hemorrhage (RH) and discerning whether the RH involved the anatomical macula, rather than a specific class of single disease. RH was diagnosed automatically by CNN (InceptionResNetV2) with 16 827 UWF images. In this study, all images were assigned to two categories, the RH and non-RH. RH category included images of various types of hemorrhages, even microaneurysms were also included, which is difficult to be distinguished from dot hemorrhages in the UWF images. The non-RH category included images of normal retinas and various retinopathies such as RD, central serous chorioretinopathy, and retinitis pigmentosa. Although they achieved great performance in classifying RH and non-RH, the limitation of removing poor-quality images and missing RH diagnoses in an obscured area of UWF images is reserved.

Diagnosis of Multiple Diseases Although DL has achieved a good performance in diagnosing a single disease, it still cannot be applied to clinical work in the real world. Because there are many ophthalmic diseases in different patients with different ophthalmic diseases that may affect each other in the process of diagnosis, such as retinal vascular disease (DR, RVO, and Coats). Using DL models to diagnosis multiple diseases may be a possible solution to this problem. which is more convenient and helpful to clinicians. Currently, the classification of UWF images for multiple diseases mainly focuses on four classification tasks, including three disease

images and a group of normal images.

Retinal tear, retinal detachment, diabetic retinopathy, and pathologic myopia In 2021, Zhang *et al*^[55] developed a set of early abnormal screening systems named DeepUWF for diagnosing for retinal tears, RD, DR, and PM with 2644 UWF images. Additionally, they proposed six kinds of image preprocessing techniques to solve the limitation of the low contrast of UWF images, which will improve the ability to extract fine features by depth model and achieve good sensitivity and specificity. Meanwhile, they found that the image optimization methods may be beneficial in improving the prediction ability of the models by adjusting the contrast, brightness, and gray level of the images and highlighting the features of the lesions and diseases. In addition, different algorithms have different prediction capabilities for each preprocessing method. In the same year, aiming to alleviate severe class imbalance and similarity between classes, Zhang *et al*^[56] proposed two-stage, and one-stage classification strategies. The one-step strategy is a five-class classification model, which was trained directly on the sign dataset that includes normal fundus images or on the disease dataset that includes normal fundus images. The two-step classification strategy contains two steps: First, binary classification models are used to distinguish between normal images and images with abnormal signs (or symptoms). At this stage, it focuses on achieving a good compromise between sensitivity and specificity. Second, the four-class classification models identify abnormal signs or diagnose retinal diseases. This phase focuses on identifying samples of minority classes in the context of class imbalance. Their experimental results show that DeepUWF-Plus is effective when using the two-stage strategy, especially for identifying signs or symptoms of minor diseases. This improves the practicality of fundus screening and enables ophthalmologists to provide more comprehensive fundus assessments.

Lattice degeneration, retinal breaks, and retinal detachment Zhang *et al*^[46] included 911-eligible UWF images to investigate the detection of lattice degeneration, retinal breaks, and RD in tessellated eyes using UWF images. They used a combined deep-learning system of 3 optimal binary classification models trained using the seResNext50 algorithm with 2 preprocessing methods (original resizing and cropping). This study preliminarily verifies the feasibility of a DL system as a screening tool to detect lattice degeneration, retinal breaks, and RD. Compared to the cropping method, the better preprocessing approach for RD and lattice degeneration is an original resizing method, while the cropping method achieved better outcomes on retinal breaks. The authors thought it might be related to the lesion size of the disease. Lesions of retinal breaks are relatively small to UWF images,

for which the cropping method enables the DL system to learn more details about lesions. In contrast, the range of RD and the size of lattice degeneration is often large enough for direct detection, and excessive irrelevant information may be augmented and interfere with the training of the DL model.

Diabetic retinopathy, retinitis pigmentosa, and Coats Xie *et al*^[57] used the ResNet-34 model as the backbone to propose a novel DL model based on UWF images for detecting different ophthalmic diseases, Coats, RP, and DR, which can extract more deep-level features of UWF images. The proposed architecture consists of a multibranch network, ASPP, depthwise and cross-attention modules. The multibranch network is based on a depthwise attention module combined with the ResNet-34 model and ASPP module. Furthermore, the cross-attention module could learn the distinction and relationship among different diseases by channel and spatial attention strategies and integrate the extracted attention map *via* cross-fusion mode to gain the relevant features of specific diseases. In this study, they conduct ablation experiments with certain modules, verifying that the devised module effectively improves the classification performance. Compared to several network structures including the single ResNet-34 model (Res34), multibranch network (MB), multibranch network with ASPP (MB-ASPP), MB-ASPP and depthwise attention module (MB-ASPP-DA) and cross-attention modules (proposed), the architecture of the multibranch network based on the ResNet-34 model was superior to that of the single ResNet-34 model, and the ASPP module also played a role in the improving the classification results. However, the small number of datasets is insufficient for a deep neural network to learn deep-level and discriminative features. The network only learns limited ophthalmic disease species, including RP, DR, and Coats.

Retinal vascular disease In 2022, Abitbol *et al*^[58] used a multilayer deep convolutional neural network (DenseNet121) to differentiate UWF images between different vascular diseases (DR, sickle cell retinopathy, and RVO) and healthy controls. In this study, 224 UWF images were included, of which 169 were of retinal vascular diseases, and 55 were healthy controls, with an overall accuracy of 88.4%. Meanwhile, they used fivefold cross-validation to evaluate the performances of the DL framework, which maximizes performances while minimizing bias of the small datasets. In Summary, they showed the feasibility of automated DL classification for detecting several retinal vascular diseases using UWF images. In the future, we need to enlarge the types of retinal vascular diseases and the number of datasets to achieve better performance.

Deep Learning Models in Ultrawide-Field Fundus Images In computer vision, CNNs have become the mainstream

approach, such as VGGNet^[59], ResNet^[60], DenseNet^[61]. In the classification tasks for the diagnosis and grading of ophthalmic disease in UWF images, VGGNet, ResNet, and DensNet are the most widely used classification backbone networks, especially the VGG-16 as shown in Tables 1 and 2.

VGGNet VGGNet was designed by the Visual Geometry Group, Department of Engineering Science, University of Oxford. It has released several convolutional network models starting with VGG-16 to VGG-19^[59]. Exploring the influence of the convolutional network depth on its precision in a wide-ranging image recognition context is their focus. A comprehensive assessment of networks of ever-growing profundity, utilizing a 3×3 convolution filter architecture and 2×2 max-pooling layers, is their primary contribution. Achieving a remarkable enhancement of the prior-art arrangements can be accomplished by increasing the depth to 16-19 weight layers. This innovation mainly brings two advantages, namely reducing the number of network parameters and improving the network's performance. First, the concatenation of two 3×3 convolutional layers is equivalent to a 5×5 convolutional layer, and the concatenation of three 3×3 convolutional layers is equivalent to a 7×7 convolutional layer, which means the receptive fields of the three 3×3 convolutional layers are equivalent in size in a 7×7 convolutional layer. At the same time, it has fewer parameters than a 7×7 convolutional layer so that the model will be smaller and the model can be designed deeper. Second, and most importantly, three 3×3 convolutional layers have more nonlinear transformations than one 7×7 convolutional layer (the former can use three ReLU activation functions, while the latter can use them only once). This gives CNN a stronger learning ability for features and a stronger nonlinear fitting ability. The block structure that reuses the same convolution kernel size multiple times is widely used after VGGNet. Because it can extract more complex and expressive features, this model is also widely used in computer-aided diagnosis of ophthalmic diseases based on medical images (CFP, UWF, OCTA, and so on). As shown in Tables 1 and 2, some DL methods based on UWF images mainly use VGGNet and achieve good performance^[48-50].

ResNet Another DL network widely used in UWF images is ResNet, designed by He *et al*^[60] from Microsoft Research. A residual learning framework is presented to facilitate the training of networks that are far more profound than those employed before. Reformulating the layers as residual functions concerning the layer inputs, instead of learning unreferenced functions, is what they do. Providing comprehensive empirical evidence, they demonstrate that optimizing residual networks is simpler and accuracy can be augmented with a greater depth. An example of this is the ImageNet dataset, where residual nets with a depth of up to

152 layers (8 times deeper than VGGNet) are evaluated, yet still of a lesser complexity. The significance of the depth of representations in numerous visual recognition tasks is made evident. As mentioned above, as the network's depth increases, the network's accuracy should increase synchronously, except for the overfitting problem. One problem with increasing network depth is propagating the gradient from back to front. After expanding the network depth, the gradient of the earlier layers will be very small. These layers are stuck in learning, which is the gradient vanishing problem. The second problem with deep networks is training. When the network is deeper, the parameter space is more extensive, and the optimization problem becomes more complicated, so simply increasing the network depth will result in higher training errors. Residual network ResNet designs a residual module that allows us to train deeper networks. In addition, traditional convolutional layers or fully connected layers have problems such as loss during information transfer. To a certain degree, ResNet resolves this issue. The integrity of the data is safeguarded by transmitting it directly to the output. The entire network is only required to comprehend a portion of the divergence between the input and output, thus simplifying the learning objectives and complexity. After using the structure of ResNet, the training error of the ResNet network gradually decreases as the number of layers increases, and the performance on the test dataset will also improve. Therefore, it is widely used as a common benchmark model in many medical image (CFP and UWF images) analysis tasks.

DenseNet The densely connected convolutional network (DenseNet) model has the same basic idea as ResNet, but it builds a dense connection between all the preceding and following layers. DenseNet departs from the stereotypical thinking of deepening the number of layers and widening the network structure to improve the network performance and consider the perspective of features^[61]. Through feature reuse and bypass settings, it not only drastically reduces the number of network parameters but also alleviates the vanishing gradient problem to a certain extent^[61]. Another highlight of DenseNet is the connection of features on the channel to achieve feature reuse. These features allow DenseNet to perform better than ResNet with fewer parameters and lower computational costs. Several other methods have been proposed to improve model performance. Deeper networks tend to perform better, but gradient dispersion is a common problem. We also need to pay attention to the large network structure parameters, the large amount of computation, and the high consumption costs. Additionally, to improve the network model's superiority, it is necessary to consider its complexity and properly adjust the convolution structure of the convolution module.

Inception and other networks To maintain the sparsity of the neural network structure and fully use the high computational performance of dense matrices, GoogleNet proposes a deep convolutional neural network architecture codenamed Inception to achieve this purpose^[62-63]. A meticulously crafted design that augments the network's computing resources has been the primary feature of this architecture, resulting in a more effective utilization of them. The computational budget is kept constant, and the depth and width remain unchanged. The Hebbian principle and multiscale processing intuition were the basis for designing architectural decisions to maximize quality. The most effective way to enhance network performance is to expand its depth and breadth. The depth of the network is denoted by the number of layers, while the width is the number of channels in each layer. Despite this, there are two drawbacks^[63]: 1) Overfitting is likely to occur. As the depth and breadth widen, the parameters to be acquired become more extensive, thus making them vulnerable to overfitting. 2) A larger network will result in a greater computational demand. Therefore, the solution to the above shortcomings is introducing sparse features and converting the fully connected layers into sparse connections. The innovation of Inception is to use different sizes of convolution kernels to process the input and then splice the obtained feature maps. The main purpose is to increase the feature diversification and improve the network adaptability. Google proposed adding the residual structure ResNet into the Inception module, fully using the identity mapping characteristics of the ResNet network structure, improving the grid accuracy, and simultaneously solving the problems of grid degradation and gradient disappearance^[64]. Some research also uses a model combining Inception and ResNet for UWF image analysis^[35,44,54]. In addition, another algorithm network based on Inception is Xception. It is improved based on Inception v3. All 3×3 modules in Inception v3 are replaced with depthwise separable convolution. This separable depth convolution can reduce many model parameters and computational complexity while retaining high accuracy^[60,64].

DISCUSSION

AI and UWF images help the realize automatic diagnosis and recognition of multiple ophthalmic diseases. Although there have been some research results for common ophthalmic diseases such as DR and glaucoma, the research on AI based on DL in UWF images is still limited and cannot be applied to clinical work. There are mainly the following reasons. First, although UWF images can provide a 200° view with an ellipsoidal mirror and can comprehensively evaluate the condition of the retina, it will lead to distortion of the UWF images, including significant warping of the retinal area, magnification of peripheral areas, and artifactual stretching

of the horizontal axis. The patient's eyelashes and tarsal gland will appear in UWF images, which will affect the key feature extraction of the images^[65]. Second, images with low image quality caused by various diseases that cause refractive medium changes will influence the identification of diseases using DL models, such as cataracts, vitreous opacity, and severe fundus hemorrhage. Currently, many low-quality images have been excluded, resulting in differences between the recognition of disease images in the real world. Naturally, some studies have used AI to automatically extract the true retinal area from UWF images based on image processing^[66-67], such as a generative adversarial network called AMD-GAN based on the attention encoder and multibranch structure for retinal disease detection from UWF images, and the prior knowledge of experts is utilized to improve the detection results^[67]. Meanwhile, a few other studies explored the effect of different preprocessing techniques for UWF images, such as original, augmented, and histogram-equalized images, which can improve the performance in detecting disease in UWF images^[45]. Third, UWF images reflect the planar features of the retina and it cannot clearly show the deep structures of the retina. It cannot correctly identify whether there is edema in the macular area and the extent of edema and other lesions in deep layers. In addition, the small sample size of UWF images is another matter in the application of DL, which is difficult to collect in the clinic because it is relatively new equipment in the clinic. Most researchers use image augmentation and transfer learning to address the problem of small training sets based on DCNN. Transfer learning fixes the lower weights optimized to recognize structures in general images using feedforward methods and retrains the upper consequences using backpropagation. The model can identify features of ophthalmological images much faster and has a significantly smaller training dataset and fewer computational requirements. The lack of data in a particular domain is addressed using images from similar domains.

Currently, UWF image-based AI for the diagnosis of ophthalmic diseases mainly focuses on unimodal images. However, in clinical work, although a unimodal image can provide a preliminary examination of a disease but cannot provide a comprehensive assessment of a patient's condition. Clinicians often need to combine information from multiple images when making accurate diagnoses and appropriate treatment decisions for various retinal diseases^[68]. Therefore, there is a need to further explore the effectiveness of AI in diagnosing multiple ophthalmic diseases in multiple modalities. For example, combining UWF images with other imaging techniques, such as OCT, FFA, OCTA, and other images. It will help in the comprehensive assessment of a patient's condition. There is also a need to develop more

flexible AI models that can input different image modalities for comprehensive diagnosis. This will be applicable in complex clinical work environments and will help in the long-term integrated and intelligent management of patients.

With the development of DL, CNNs have become the main algorithmic model for disease diagnosis, and the depth and complexity of CNNs have been increasing to achieve superior performance. However, this will lead to the need to consume a large amount of storage space and arithmetic resources. Large network models such as VGG16, ResNet152, and DenseNet121 are accompanied by a large number of model parameters and computations during the training process, which makes it difficult to run on mobile devices or embedded platforms. Therefore, it is important to study lightweight CNNs, such as shuffleNet^[69], MobileNet^[70], GhostNet^[71], *etc.* On the basis of guaranteeing accuracy, the model parameters and computation amount are reduced to balance the performance and efficiency. Among the many studies investigating the combination of DL and UWF imaging modalities, the main model used is the VGG16 network model, and the performance of the lightweight network model for diagnostic recognition of ophthalmic diseases can be further explored.

The critical factors for the success of DL are that the network is deep enough, the connections are complex enough, and the nonlinear combination of activation functions allows feature extraction from raw data at any level. However, these advantages lead to a lack of interpretability of DL: one cannot understand the logic underlying the decisions made by the "black box" model and cannot judge the reliability of the algorithm's decisions. Some studies visualized the DL systems in detecting disease with heatmaps to explain the rationale of DL. Similarly, Kermany *et al*^[72] used the occlusion test to identify the areas of greatest importance used by the DL model in assigning a diagnosis of AMD and identified the most clinically significant regions of pathology. In addition, interpretative algorithms allow network users to better understand the network's strengths and weaknesses. Interpretative algorithms are crucial to the future development, debugging, and widespread deployment of DL models. Therefore, it should enhance subsequent research on applying interpretive algorithms in ophthalmology. Regarding the research process, some studies take an isolated approach to assessing DL diagnostic accuracy, and there is a lack of consensus on a principled approach to calculating the sample size required to train DL models^[73]. The metric parameters reflecting model performance are not uniform, and the selection of thresholds lacks standards. The above issues suggest the need for continuous improvement in follow-up.

CONCLUSION

From CFP to UWF images, the advancement of equipment provides more information on ophthalmic disease. With the development of DL, AI has made significant accomplishments in diagnosing ophthalmic disease with UWF images, which will be used in clinical practice broadly and significantly impact the medical and ophthalmology community to benefit people from least developed countries and regions in the future.

ACKNOWLEDGEMENTS

Authors' contributions: Tang QQ and Yang XG conceived experiments, analyzed the data, prepared figures and tables, write the manuscript of the paper. Wang HQ and Wu DW performed the experiments and contributed analysis tools. Zhang MX authored and reviewed drafts of the paper and approved the final draft.

Foundation: Supported by 1.3.5 Project for Disciplines of Excellence, West China Hospital, Sichuan University (No. ZYJC21025).

Conflicts of Interest: Tang QQ, None; Yang XG, None; Wang HQ, None; Wu DW, None; Zhang MX, None.

REFERENCES

- Williams LB, Prakalapakorn SG, Ansari Z, Goldhardt R. Impact and trends in global ophthalmology. *Curr Ophthalmol Rep* 2020;8(3):136-143.
- Lee R, Wong TY, Sabanayagam C. Epidemiology of diabetic retinopathy, diabetic macular edema and related vision loss. *Eye Vis (Lond)* 2015;2:17.
- Saeedi P, Petersohn I, Salpea P, et al. Global and regional diabetes prevalence estimates for 2019 and projections for 2030 and 2045: results from the International Diabetes Federation Diabetes Atlas, 9th edition. *Diabetes Res Clin Pract* 2019;157:107843.
- Wong WL, Su X, Li X, Cheung CM, Klein R, Cheng CY, Wong TY. Global prevalence of age-related macular degeneration and disease burden projection for 2020 and 2040: a systematic review and meta-analysis. *Lancet Glob Health* 2014;2(2):e106-e116.
- Tham YC, Li X, Wong TY, Quigley HA, Aung T, Cheng CY. Global prevalence of glaucoma and projections of glaucoma burden through 2040. *Ophthalmology* 2014;121(11):2081-2090.
- Holden BA, Fricke TR, Wilson DA, Jong M, Naidoo KS, Sankaridurg P, Wong TY, Naduvilath TJ, Resnikoff S. Global prevalence of myopia and high myopia and temporal trends from 2000 through 2050. *Ophthalmology* 2016;123(5):1036-1042.
- Li B, Chen H, Zhang BL, et al. Development and evaluation of a deep learning model for the detection of multiple fundus diseases based on colour fundus photography. *Br J Ophthalmol* 2022;106(8):1079-1086.
- Pascal L, Perdomo OJ, Bost X, Huet B, Otálora S, Zuluaga MA. Multi-task deep learning for glaucoma detection from color fundus images. *Sci Rep* 2022;12(1):12361.
- Chueh KM, Hsieh YT, Chen HH, Ma IH, Huang SL. Identification of sex and age from macular optical coherence tomography and feature analysis using deep learning. *Am J Ophthalmol* 2022;235:221-228.
- You QS, Tsuboi K, Guo Y, Wang J, Flaxel CJ, Bailey ST, Huang D, Jia Y, Hwang TS. Comparison of central macular fluid volume with central subfield thickness in patients with diabetic macular edema using optical coherence tomography angiography. *JAMA Ophthalmol* 2021;139(7):734-741.
- Wang J, Hormel TT, Gao L, Zang P, Guo Y, Wang X, Bailey ST, Jia Y. Automated diagnosis and segmentation of choroidal neovascularization in OCT angiography using deep learning. *Biomed Opt Express* 2020;11(2):927-944.
- Gao Z, Jin K, Yan Y, et al. End-to-end diabetic retinopathy grading based on fundus fluorescein angiography images using deep learning. *Graefes Arch Clin Exp Ophthalmol* 2022;260(5):1663-1673.
- Nagasawa T, Tabuchi H, Masumoto H, Morita S, Niki M, Ohara Z, Yoshizumi Y, Mitamura Y. Accuracy of diabetic retinopathy staging with a deep convolutional neural network using ultra-wide-field fundus ophthalmoscopy and optical coherence tomography angiography. *J Ophthalmol* 2021;2021:6651175.
- Grassmann F, Mengelkamp J, Brandl C, Harsch S, Zimmermann ME, Linkohr B, Peters A, Heid IM, Palm C, Weber BHF. A deep learning algorithm for prediction of age-related eye disease study severity scale for age-related macular degeneration from color fundus photography. *Ophthalmology* 2018;125(9):1410-1420.
- Schlegl T, Waldstein SM, Bogunovic H, Endstraßer F, Sadeghipour A, Philip AM, Podkowinski D, Gerendas BS, Langs G, Schmidt-Erfurth U. Fully automated detection and quantification of macular fluid in OCT using deep learning. *Ophthalmology* 2018;125(4):549-558.
- Seebock P, Orlando JI, Schlegl T, Waldstein SM, Bogunovic H, Klimescha S, Langs G, Schmidt-Erfurth U. Exploiting epistemic uncertainty of anatomy segmentation for anomaly detection in retinal OCT. *IEEE Trans Med Imaging* 2020;39(1):87-98.
- Lo YC, Lin KH, Bair H, Sheu WH, Chang CS, Shen YC, Hung CL. Epiretinal membrane detection at the ophthalmologist level using deep learning of optical coherence tomography. *Sci Rep* 2020;10(1):8424.
- Xiao Y, Hu Y, Quan W, et al. Development and validation of a deep learning system to classify aetiology and predict anatomical outcomes of macular hole. *Br J Ophthalmol* 2023;107(1):109-115.
- Li Y, Feng W, Zhao X, et al. Development and validation of a deep learning system to screen vision-threatening conditions in high myopia using optical coherence tomography images. *Br J Ophthalmol* 2022;106(5):633-639.
- Haleem MS, Han L, van Hemert J, Li BH, Fleming A. Retinal area detector from scanning laser ophthalmoscope (SLO) images for diagnosing retinal diseases. *IEEE J Biomed Health Inform* 2014;19(4):1472-1482.
- Nagieli A, Lalane RA, Sadda SR, Schwartz SD. Ultra-widefield fundus imaging: a review of clinical applications and future trends. *Retina* 2016;36(4):660-678.
- Nagasato D, Tabuchi H, Masumoto H, Kusuyama T, Yu KW, Ishitobi N, Furukawa H, Adachi S, Murao F, Mitamura Y. Prediction of age

- and brachial-ankle pulse-wave velocity using ultra-wide-field pseudo-color images by deep learning. *Sci Rep* 2020;10(1):19369.
- 23 Wilkinson CP, Ferris FL, Klein RE, Lee PP, Agardh CD, Davis M, Dills D, Kambik A, Pararajasegaram R, Verdager JT. Proposed international clinical diabetic retinopathy and diabetic macular edema disease severity scales. *Ophthalmology* 2003;110(9):1677-1682.
- 24 Early photocoagulation for diabetic retinopathy. ETDRS report number 9. Early Treatment Diabetic Retinopathy Study Research Group. *Ophthalmology* 1991;98(5 Suppl):766-785.
- 25 Li T, Bo W, Hu C, Kang H, Liu H, Wang K, Fu H. Applications of deep learning in fundus images: a review. *Med Image Anal* 2021;69:101971.
- 26 Wang S, Zhang Y, Lei S, Zhu H, Li J, Wang Q, Yang J, Chen S, Pan H. Performance of deep neural network-based artificial intelligence method in diabetic retinopathy screening: a systematic review and meta-analysis of diagnostic test accuracy. *Eur J Endocrinol* 2020;183(1):41-49.
- 27 Wu L, Fernandez-Loaiza P, Sauma J, Hernandez-Bogantes E, Masis M. Classification of diabetic retinopathy and diabetic macular edema. *World J Diabetes* 2013;4(6):290-294.
- 28 Nagasawa T, Tabuchi H, Masumoto H, Enno H, Niki M, Ohara Z, Yoshizumi Y, Ohsugi H, Mitamura Y. Accuracy of ultrawide-field fundus ophthalmoscopy-assisted deep learning for detecting treatment-naïve proliferative diabetic retinopathy. *Int Ophthalmol* 2019;39(10):2153-2159.
- 29 Oh K, Kang HM, Leem D, Lee H, Seo KY, Yoon S. Early detection of diabetic retinopathy based on deep learning and ultra-wide-field fundus images. *Sci Rep* 2021;11(1):1897.
- 30 Wang K, Jayadev C, Nittala MG, Velaga SB, Ramachandra CA, Bhaskaranand M, Bhat S, Solanki K, Sadda SR. Automated detection of diabetic retinopathy lesions on ultrawidefield pseudocolour images. *Acta Ophthalmol* 2018;96(2):e168-e173.
- 31 Olvera-Barrios A, Heeren TF, Balaskas K, Chambers R, Bolter L, Egan C, Tufail A, Anderson J. Diagnostic accuracy of diabetic retinopathy grading by an artificial intelligence-enabled algorithm compared with a human standard for wide-field true-colour confocal scanning and standard digital retinal images. *Br J Ophthalmol* 2021;105(2):265-270.
- 32 Wu Y, Szymanska M, Hu Y, Fazal MI, Jiang N, Yetisen AK, Cordeiro MF. Measures of disease activity in glaucoma. *Biosens Bioelectron* 2022;196:113700.
- 33 Masumoto H, Tabuchi H, Nakakura S, Ishitobi N, Miki M, Enno H. Deep-learning classifier with an ultrawide-field scanning laser ophthalmoscope detects glaucoma visual field severity. *J Glaucoma* 2018;27(7):647-652.
- 34 Tabuchi H, Masumoto H, Nakakura S, Noguchi A, Tanabe H. Discrimination ability of glaucoma via DCNNs models from ultra-wide angle fundus images comparing either full or confined to the optic disc. In: Carneiro G, You S. (eds) *Computer Vision-ACCV 2018 Workshops*. Springer, Cham; 2019:229-234.
- 35 Li Z, Guo C, Lin D, et al. Deep learning for automated glaucomatous optic neuropathy detection from ultra-widefield fundus images. *Br J Ophthalmol* 2021;105(11):1548-1554.
- 36 Shin Y, Cho H, Shin YU, Seong M, Choi JW, Lee WJ. Comparison between deep-learning-based ultra-wide-field fundus imaging and true-colour confocal scanning for diagnosing glaucoma. *J Clin Med* 2022;11(11):3168.
- 37 Thomas CJ, Mirza RG, Gill MK. Age-related macular degeneration. *Med Clin North Am* 2021;105(3):473-491.
- 38 Colijn JM, Buitendijk GHS, Prokofyeva E, et al. Prevalence of age-related macular degeneration in Europe: the past and the future. *Ophthalmology* 2017;124(12):1753-1763.
- 39 Rasmussen A, Bloch SB, Fuchs J, Hansen LH, Larsen M, LaCour M, Lund-Andersen H, Sander B. A 4-year longitudinal study of 555 patients treated with ranibizumab for neovascular age-related macular degeneration. *Ophthalmology* 2013;120(12):2630-2636.
- 40 Matsuba S, Tabuchi H, Ohsugi H, Enno H, Ishitobi N, Masumoto H, Kiuchi Y. Accuracy of ultra-wide-field fundus ophthalmoscopy-assisted deep learning, a machine-learning technology, for detecting age-related macular degeneration. *Int Ophthalmol* 2019;39(6):1269-1275.
- 41 Tak N, Reddy AJ, Martel J, Martel JB. Clinical wide-field retinal image deep learning classification of exudative and non-exudative age-related macular degeneration. *Cureus* 2021;13(8):e17579.
- 42 Heussen N, Feltgen N, Walter P, Hoerauf H, Hilgers RD, Heimann H; SPR Study Group. Scleral buckling versus primary vitrectomy in rhegmatogenous retinal detachment study (SPR Study): predictive factors for functional outcome. Study report no. 6. *Graefes Arch Clin Exp Ophthalmol* 2011;249(8):1129-1136.
- 43 Ohsugi H, Tabuchi H, Enno H, Ishitobi N. Accuracy of deep learning, a machine-learning technology, using ultra-wide-field fundus ophthalmoscopy for detecting rhegmatogenous retinal detachment. *Sci Rep* 2017;7(1):9425.
- 44 Li Z, Guo C, Nie D, et al. Deep learning for detecting retinal detachment and discerning macular status using ultra-widefield fundus images. *Commun Biol* 2020;3(1):15.
- 45 Li Z, Guo C, Nie D, et al. A deep learning system for identifying lattice degeneration and retinal breaks using ultra-widefield fundus images. *Ann Transl Med* 2019;7(22):618.
- 46 Zhang C, He F, Li B, Wang H, He X, Li X, Yu W, Chen Y. Development of a deep-learning system for detection of lattice degeneration, retinal breaks, and retinal detachment in tessellated eyes using ultra-wide-field fundus images: a pilot study. *Graefes Arch Clin Exp Ophthalmol* 2021;259(8):2225-2234.
- 47 Song P, Xu Y, Zha M, Zhang Y, Rudan I. Global epidemiology of retinal vein occlusion: a systematic review and meta-analysis of prevalence, incidence, and risk factors. *J Glob Health* 2019;9(1):010427.
- 48 Nagasato D, Tabuchi H, Ohsugi H, Masumoto H, Enno H, Ishitobi N, Sonobe T, Kameoka M, Niki M, Hayashi K, Mitamura Y. Deep neural network-based method for detecting central retinal vein occlusion using ultrawide-field fundus ophthalmoscopy. *J Ophthalmol* 2018;2018:1875431.

- 49 Nagasato D, Tabuchi H, Ohsugi H, Masumoto H, Enno H, Ishitobi N, Sonobe T, Kameoka M, Niki M, Mitamura Y. Deep-learning classifier with ultrawide-field fundus ophthalmoscopy for detecting branch retinal vein occlusion. *Int J Ophthalmol* 2019;12(1):94-99.
- 50 Masumoto H, Tabuchi H, Nakakura S, Ohsugi H, Enno H, Ishitobi N, Ohsugi E, Mitamura Y. Accuracy of a deep convolutional neural network in detection of retinitis pigmentosa on ultrawide-field images. *PeerJ* 2019;7:e6900.
- 51 Song DJ, Bao XL, Fan B, Li GY. Mechanism of cone degeneration in retinitis pigmentosa. *Cell Mol Neurobiol* 2022;43:1037-1048.
- 52 Liew G, Strong S, Bradley P, Severn P, Moore AT, Webster AR, Mitchell P, Kifley A, Michaelides M. Prevalence of cystoid macular oedema, epiretinal membrane and cataract in retinitis pigmentosa. *Br J Ophthalmol* 2019;103(8):1163-1166.
- 53 Nagasawa T, Tabuchi H, Masumoto H, Enno H, Niki M, Ohsugi H, Mitamura Y. Accuracy of deep learning, a machine learning technology, using ultra-wide-field fundus ophthalmoscopy for detecting idiopathic macular holes. *PeerJ* 2018;6:e5696.
- 54 Li Z, Guo C, Nie D, et al. Development and evaluation of a deep learning system for screening retinal hemorrhage based on ultra-widefield fundus images. *Transl Vis Sci Technol* 2020;9(2):3.
- 55 Zhang W, Zhao X, Chen Y, Zhong J, Yi Z. DeepUWF: an automated ultra-wide-field fundus screening system via deep learning. *IEEE J Biomed Health Inform* 2021;25(8):2988-2996.
- 56 Zhang W, Dai Y, Liu M, Chen Y, Zhong J, Yi Z. DeepUWF-plus: automatic fundus identification and diagnosis system based on ultrawide-field fundus imaging. *Applied Intelligence* 2021;51:7533-7551.
- 57 Xie H, Zeng X, Lei H, Du J, Wang J, Zhang G, Cao J, Wang T, Lei B. Cross-attention multi-branch network for fundus diseases classification using SLO images. *Med Image Anal* 2021;71:102031.
- 58 Abitbol E, Miere A, Excoffier JB, Mehanna CJ, Amoroso F, Kerr S, Ortala M, Souied EH. Deep learning-based classification of retinal vascular diseases using ultra-widefield colour fundus photographs. *BMJ Open Ophthalmol* 2022;7(1):e000924.
- 59 Simonyan K, Zisserman A. Very deep convolutional networks for large-scale image recognition. 2014:arXiv: 1409.1556. <https://arxiv.org/abs/1409.1556.pdf>
- 60 He K, Zhang X, Ren S, Sun J. Deep residual learning for image recognition. *2016 IEEE Conference on Computer Vision and Pattern Recognition (CVPR)*. Las Vegas, NV, USA. IEEE, 2016:770-778.
- 61 Huang G, Liu Z, van der Maaten L, Weinberger KQ, IEEE. Densely Connected Convolutional Networks. *2017 IEEE Conference on Computer Vision and Pattern Recognition (CVPR)*. Honolulu, HI, USA. IEEE, 2017:2261-2269.
- 62 Szegedy C, Liu W, Jia YQ, Sermanet P, Reed S, Anguelov D, Erhan D, Vanhoucke V, Rabinovich A. Going deeper with convolutions. *2015 IEEE Conference on Computer Vision and Pattern Recognition (CVPR)*. Boston, MA, USA. IEEE, 2015:1-9.
- 63 Szegedy C, Vanhoucke V, Ioffe S, Shlens J, Wojna Z. Rethinking the inception architecture for computer vision. *2016 IEEE Conference on Computer Vision and Pattern Recognition (CVPR)*. Las Vegas, NV, USA. IEEE, 2016:2818-2826.
- 64 Szegedy C, Ioffe S, Vanhoucke V, Alemi A. Inception-v4, inception-ResNet and the impact of residual connections on learning. *AAAI'17: Proceedings of the Thirty-First AAAI Conference on Artificial Intelligence* 2017:4278-4284.
- 65 Zhao X, Meng L, Su H, Lv B, Lv C, Xie G, Chen Y. Deep-learning-based hemoglobin concentration prediction and anemia screening using ultra-wide field fundus images. *Front Cell Dev Biol* 2022;10:888268.
- 66 Tang F, Luenam P, Ran AR, et al. Detection of diabetic retinopathy from ultra-widefield scanning laser ophthalmoscope images: a multicenter deep learning analysis. *Ophthalmol Retina* 2021;5(11):1097-1106.
- 67 Xie H, Lei H, Zeng X, He Y, Chen G, Elazab A, Yue G, Wang J, Zhang G, Lei B. AMD-GAN: attention encoder and multi-branch structure based generative adversarial networks for fundus disease detection from scanning laser ophthalmoscopy images. *Neural Netw* 2020;132:477-490.
- 68 Kang EY, Yeung L, Lee YL, Wu CH, Peng SY, Chen YP, Gao QZ, Lin C, Kuo CF, Lai CC. A multimodal imaging-based deep learning model for detecting treatment-requiring retinal vascular diseases: model development and validation study. *JMIR Med Inform* 2021;9(5):e28868.
- 69 Wang JZ, Lu NH, Du WC, Liu KY, Hsu SY, Wang CY, Chen YJ, Chang LC, Twan WH, Chen TB, Huang YH. Classification of color fundus photographs using fusion extracted features and customized CNN models. *Healthcare (Basel)* 2023;11(15):2228.
- 70 Sandler M, Howard A, Zhu ML, Zhmoginov A, Chen LC. MobileNetV2: inverted residuals and linear bottlenecks. *2018 IEEE/CVF Conference on Computer Vision and Pattern Recognition (CVPR)*. Salt Lake City, UT, USA. IEEE, 2018:4510-4520.
- 71 Han K, Wang Y, Tian Q, Guo JY, Xu CJ, Xu C. GhostNet: more features from cheap operations. *2020 IEEE/CVF Conference on Computer Vision and Pattern Recognition (CVPR)*. Seattle, WA, USA. IEEE, 2020:1577-1586.
- 72 Kermansy DS, Goldbaum M, Cai W, et al. Identifying medical diagnoses and treatable diseases by image-based deep learning. *Cell* 2018;172(5):1122-1131.e9.
- 73 Liu X, Faes L, Kale AU, et al. A comparison of deep learning performance against health-care professionals in detecting diseases from medical imaging: a systematic review and meta-analysis. *Lancet Digit Health* 2019;1(6):e271-e297.